Diagnostics in Ocular Imaging

Cornea, Retina, Glaucoma and Orbit

Mehrdad Mohammadpour
Editor

Springer

Diagnostics in Ocular Imaging

Mehrdad Mohammadpour
Editor

Diagnostics in Ocular Imaging

Cornea, Retina, Glaucoma and Orbit

Springer

Editor
Mehrdad Mohammadpour
Farabi Eye Hospital
Tehran University of Medical Sciences
Tehran, Iran

ISBN 978-3-030-54862-9 ISBN 978-3-030-54863-6 (eBook)
https://doi.org/10.1007/978-3-030-54863-6

This Springer imprint is published by the registered company Springer Nature Switzerland AG
The registered company address is: Gewerbestrasse 11, 6330 Cham, Switzerland

Thanks to my Compassionate God for all his helps in all aspects of my life from creature to present and for teaching the human being to write their experiences.

To my Parents and Teachers who learned me gratis from the very beginning to the present time.

To my Wife Prof. Maryam Hassanzad for her patients and inexhaustible encourage as a real angel during all this 25 years of common life.

To my Students: Past, Present and future who let me transfer my knowledge to make change in their behavior to help those who need their services.

& finally
To my patients who let me be their physician and to get this expertise.

Foreword

It is my honor to write the foreword for this new book, *Diagnostics in Ocular Imaging: Cornea, Retina, Glaucoma and Orbit*. I congratulate my colleague Dr. Mehrdad Mohammadpour who spearheaded this collaborative endeavor and all contributors, especially Dr. Fedra Hajizadeh, Dr. Sasan Moghimi and Dr. Mohammad Taher Rajabi for providing an outstanding resource for the scientific community.

The rapid technological advances in recent decades have provided us with increasingly more reliable and high-resolution visualization of ocular structures, and ocular imaging has become an integral part of the daily ophthalmic practice for performing screening and diagnostic tests and monitoring responses to treatment. *Diagnostics in Ocular Imaging: Cornea, Retina, Glaucoma and Orbit* is a comprehensive atlas that introduces the reader to the state-of-the-art imaging modalities including computerized corneal topographers, corneal biomechanics analyzers, ultrasound biomicroscopes, aberrometers, optical coherence tomographers and angiographers. Throughout this well-conceived book, which is nicely organized in five main parts and 30 interesting chapters, there are illustrations and fascinating cases that keep the reader engaged regardless of their subspecialty or level of expertise.

Diagnostics in Ocular Imaging: Cornea, Retina, Glaucoma and Orbit is a welcome addition to the libraries of every eye care practitioner and an absolute must-have resource for professionals in the field of ophthalmology. I highly recommend this book as a definitive learning resource to all, especially our residents and fellows in training.

Hassan Hashemi, M.D.
Professor of Ophthalmology, Department of Ophthalmology Farabi Eye Hospital, Tehran University of Medical Sciences Tehran, Iran

Preface

It is a great honor for me to introduce this comprehensive book entitled *Diagnostics in Ocular Imaging; Cornea, Retina, Glaucoma and Orbit* which covers nicely all four major subspecialties of ophthalmology that needs ocular imaging before any major diagnosis or intervention.

Nowadays, computerized imaging has become the cornerstone and sin qua none component for diagnosis and treatment both in medical and surgical fields of ophthalmology.

This book has both benefits of a Textbook and an Atlas with introducing not only the common and routine daily practice but also challenging and rare cases that one would encounter in his or her lifelong carrier in all fields of Ophthalmology.

Another major outstanding feature of this book is its potential for training ophthalmology Residents and Fellows in all ocular fields and its future role to be considered as a Reference for Board Examinations.

Therefore, it can benefit not only the postgraduate ophthalmologists in all ocular fields but also is a great help for all ophthalmic trainees.

I cordially thank all the authors for their fantastic contribution in composing all 30 well-organized chapters covering all fields of ophthalmology and updates on emerging technologies of new devices for ocular imaging in detail.

I eagerly wait for the readers' feedbacks, opinions and their constructive reviews for considering them for next editions of the book and hope my colleagues find it helpful in their daily practice.

Best Wishes

Mehrdad Mohammadpour, M.D.
Professor of Ophthalmology, Farabi Excellence
Center of Ophthalmology and Eye Hospital
Tehran University of Medical
Sciences, Tehran, Iran

Contents

Corneal Imaging: Topography Versus Tomography

Topographic Pattern Recognition: Normal Versus Keratoconus

Sepehr Feizi

Introduction

Two-thirds of the ocular refractive power is contributed by cornea. The majority of refraction takes place at the air-tear film interface due to the maximum difference in the refractive index between air and tear film. Therefore, the shape of the anterior corneal surface plays a major role in the formation of retinal images. The posterior corneal surface has a lower radius of curvature and is steeper as compared to the anterior surface. The refractive power of posterior corneal surface is −6.0 D because the refractive index of the corneal stroma (1.376) is greater than that of the aqueous humor (1.373); therefore, the light diverges as it passes from the corneal stroma to the aqueous humor. The summation of refractive power of the anterior and posterior corneal surfaces provides a total corneal power of approximately 43.5 D at the corneal center.

True refractive power of an optical system is the summation of the refractive power of each elements. The power of each refractive surface is calculated according to the following formula:

$$P = n2 - n1/r$$

where n1 and n2 are refractive indices surrounding the refractive surface and r is the radius of curvature of this surface. The refractive power of the anterior corneal surface can be measured using a Placido disc-based corneal topographer which determines the radius of curvature of this surface. However, this device is unable to measure the refractive power of the posterior corneal surface. To consider the effect of refractive power of the posterior cornea, standard keratometric index (1.3375) rather than true corneal refractive index (1.373) is used by the

S. Feizi (✉)
Shahid Beheshti University of Medical Sciences, Tehran, Iran
e-mail: sepehrfeizi@yahoo.com

M. Mohammadpour (ed.), *Diagnostics in Ocular Imaging*,
https://doi.org/10.1007/978-3-030-54863-6_1

topographers to estimate the total corneal power. For example, a cornea with a radius of curvature of 7.7 mm in the anterior surface has an approximate power of 43.83 D (337.5/7.7).

Corneal Asphericity

Cornea is considered spheric at the central 4-mm area. Beyond this area, it takes an aspheric shape which means the corneal power decreases from the center to the periphery. This feature provide a prolate profile for the cornea. In some conditions, like after refractive surgeries performed for the correction of myopia, the dioptric power of the corneal is lower in the central area than that in the peripheral area, producing an oblate profile. Table 1 provides the asphericity values (Q values) which determine how corneal asphericity changes from the center to the periphery.

Astigmatism

Astigmatism is caused by unequal corneal powers at different meridians resulting in the formation of two or more focal lines from a point object. Astigmatism is divided into regular and irregular. The corneal power changes regularly from flat meridian to steep meridian in regular astigmatism, whereas changes in corneal power between different meridians have no consistent patterns in irregular astigmatism. Based on the orientation of the steep meridian, regular astigmatism is further categorized into with-the-rule, against-the-rule, and oblique astigmatism. The orientation of the steep meridian is between 60 and 120 degrees in with-the-rule astigmatism and between 0 and 30 degrees or 150 and 180 degrees in against-the-rule astigmatism. In oblique astigmatism, the orientation of two principle meridians is neither horizontal nor vertical.

Table 1 Asphericity (Q) values of different corneas

Asphericity	Shape	Description	Example
>0	Oblate	Cornea is flatter in the central area as compared to the peripheral area	After refractive surgeries for the correction of myopia
0	Spherical	Similar curvature at the center and periphery	Ball
$-0.26 \leq Q < 0$	Prolate	Cornea is steeper at the central area as compared to the peripheral area	Normal cornea
<-0.26	Hyperprolate	Cornea is abnormally steep in the central area	Keratoconus and after refractive surgeries performed for the correction of hyperopia

Principles of Placido Disc-Based Topography

In this technique of corneal imaging, the Placido disc is used to project a set of concentric rings on the cornea, and the shape of the corneal surface is characterized by assessing the reflection of rings off the anterior corneal surface. The corneal curvature and power are directly calculated from the data of thousands of points on the rings via sophisticated algorithms. Based on the type of the Placido discs, there are two types of topographers: topographers that use small-cone Placido disc and those that use large-cone Placido disc. Both types of topographers project a series of concentric rings of light on the anterior corneal surface. Small-cone Placido disc topographers have some advantages over large-cone Placido disc topographers including projection of more rings on the cornea and having a shorter working distance. Therefore, small-cone Placido disc systems provide a large number of measurement points and can provide more accurate data of the corneal periphery. However, these systems require a steady hand to ensure that the data acquisition is accurate. The Magellan Mapper (Nidek), Medmont E300 (Medmont), and Scout and Keratron (EyeQuip) are prototypes of small-cone topography systems. Large-cone Placido disc systems project fewer rings onto the cornea and have a longer working distance as compared to small-cone topographers. The longer working distance can mitigate the detrimental effects of eye misalignment on the accuracy of data; however, this longer distance results in the obscuration of the corneal periphery due to the shadow of nose and eyebrows (Fig. 1). Prototypes of large-cone topographers are the ReSeeVit (Veatch Ophthalmic Instruments), ATLAS 995 and 9000 (CarlZeiss Meditec), and Tomey (Computed Anatomy TMS-1).

Color Scale Settings

Different color scales are used in corneal topography maps to exhibit curvature data; areas with greater power are illustrated in warm colors including red and orange, whereas areas with lower power are depicted in cool colors including green and blue. Topographers use two different scales to display color maps including “normalized” and “absolute (or standard)” scales. The normalized scale displays the range of color codes calculated from the specific map(s). In this scale, the software determines the lowest and the highest power of the evaluated cornea and then, uses a determined number of color codes to display the map. These color codes adapt to the range of powers on the corneal surface and vary for each cornea. This scale provides an excellent general view of the entire cornea, as the scale shows the flattest to steepest readings. The same map plotted with a different scale or a different step size looks very different; relative scales or large step sizes mask characteristic patterns of irregular astigmatism (i.e. keratoconus), while small step sizes tend to exaggerate normal patterns to appear like abnormal ones (Fig. 2).

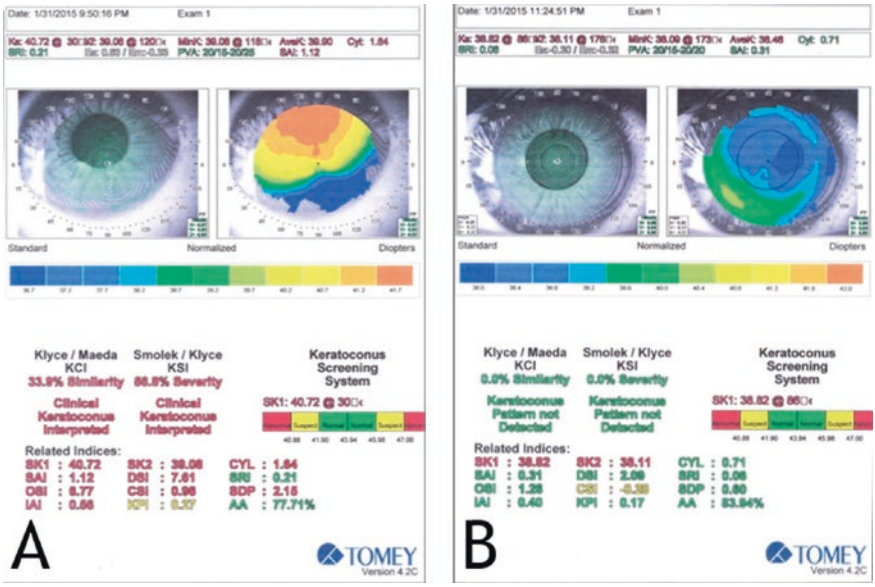

Fig. 1 Effects of the subject's fixation on the results of corneal topography. **a** Upward rotation of the eye. The topographic pattern and indices suggest that the subject has keratoconus. **b** Central fixation. Appropriate fixation of the same subject results in the normalization of all parameters. Note, the subject has undergone corneal refractive surgery and the central cornea is flatter than the peripheral area (oblate profile). The shadow of eyelashes obscures the peripheral zone of the image

The absolute (standard) scale shows a fixed range of color codes selected in the settings of the topographer irrespective of the map selected. The dioptric range, step size and number of colors are constant with this scale which allows for easier comparison to other examinations (Fig. 2).

Axial Map

The axial or sagittal map, the most common map used, displays the curvature of the anterior corneal surface in relation to the visual axis. This map, which gives an average picture (i.e. smoother appearance) of the anterior corneal curvature and is mainly used for screening, allows to correlate the anterior surface shape to the subject's refractive status. In this map, the cornea is considered as a sphere and the distance between a defined point and visual axis determines the radius of curvature of the cornea at that point. The drawback of this map is its inability to evaluate subtle changes in the corneal curvature, especially at the corneal periphery (Figs. 3 and 4).

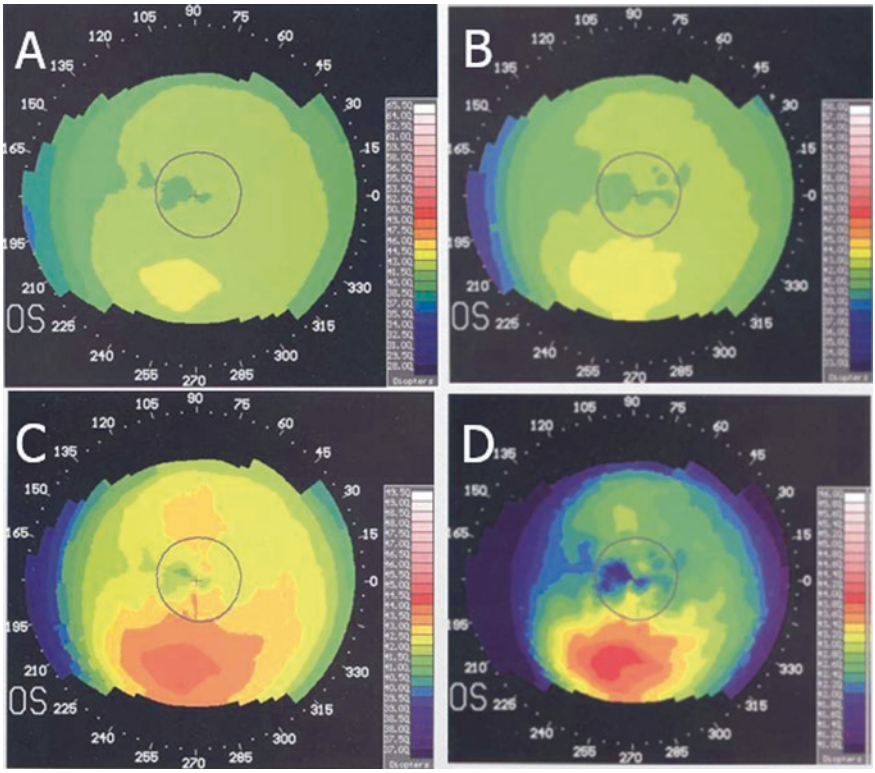

Fig. 2 Effect of different step sizes (**a**: 1.0 D, **b**: 0.75 D, **c**: 0.50 D, and **d**: 0.25 D) on the topographic pattern. An absolute scale is used to depict a cornea with keratoconus. The range of color codes used in the scale is wider than that used in the map. As indicated, large step sizes (**a** and **b**) mask an inferior steepening pattern in a keratoconus-affected cornea, whereas small step sizes (**c** and **d**) exaggerate this pattern

Tangential Map

The tangential or instantaneous map calculates each measured point of data at a 90° "tangent" to its surface and provides a more detailed description of the corneal shape, especially at the corneal periphery. Therefore, this map can define small curvature changes and provide a clearer view of the anterior surface curvatures in corneal pathologies like keratoconus. This feature is very useful to localize the size and location of corneal pathologies which can be used for the diagnosis of corneal diseases and determining an appropriate treatment plan such as the ideal lens design and the position of the intrastromal corneal ring segments for the treatment of keratoconus. Although the tangential or instantaneous map shows true radius of curvature data at each point, it appears more noisy/irregular (Fig. 3).

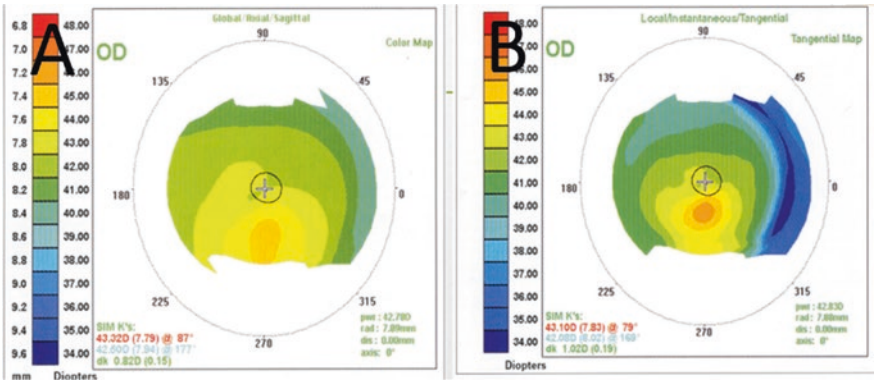

Fig. 3 Comparison of axial (**a**) and tangential (**b**) map of the same cornea. The tangential map provides a more detailed description of the corneal shape (**b**)

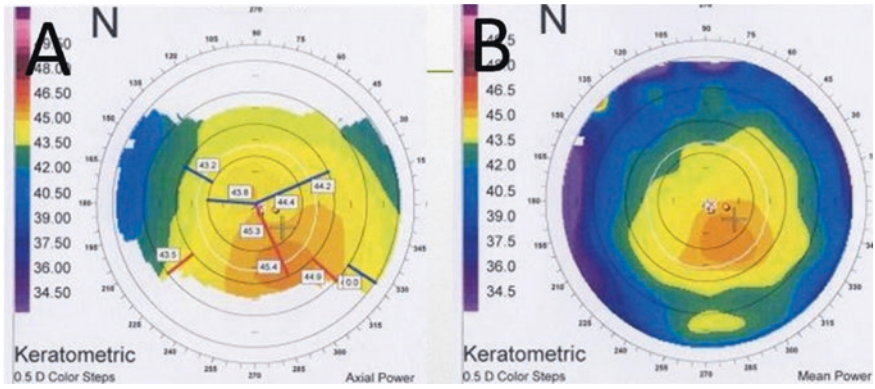

Fig. 4 Comparison of axial (**a**) and refractive power (**b**) map of the same cornea. The refractive power map demonstrates the quality of the retinal image produced by this cornea (**b**)

Refractive Power Map

The refractive power (mean power) map determines the quality of vision a subject may achieve from the corneal surface throughout the pupillary zone (Fig. 4). Refractive power maps are less commonly used but are most helpful for understanding the imaging power of the cornea and analyzing surgical effects; more uniform refractive power within the entrance pupil indicates the better ability of the anterior corneal surface to refract light properly. The drawback of this map is that it does not provide information on the shape of the anterior corneal surface.

However, this map is very effective for the interpretation of the quality of vision attainable from a subject's anterior corneal surface. For example, when comparing preoperative and postoperative corneal reshaping procedures, the refractive map demonstrates the extent that corneal surface alters contribute to the subject's quality of vision.

Elevation Map

The elevation map determines the height of the cornea in relation to the sphere that best matches the average curvature of the cornea (best fit sphere). Placido disc topography systems do not actually measure elevation; instead, they use sophisticated algorithms to extrapolate elevation data by reconstructing actual curvature. The elevation data which are represented in microns indicate the difference between the actual corneal surface and the best-fit reference sphere.

Indications

Advances in digital photography and computer processing have vastly increased the utility of corneal topography. Corneal topography is indicated for the screening of refractive surgery candidates; diagnosis of corneal diseases including keratoconus, pellucid marginal degeneration, terrien marginal degeneration; contact lens fit; evaluation of the effect of surgical interventions including corneal collagen crosslink and intrastromal corneal ring segment implantation; and selective suture removal after corneal transplantation. This diagnosis device is also used for the monitoring of the corneal disease progression.

Nomenclature of Keratoconus

Different terms are used to refer to the different stages of keratoconus. Three terms are widely used in the literature for the earliest stage of the diseases, including forme fruste keratoconus, preclinical or subclinical keratoconus, and keratoconus suspect. One needs to differentiate the early stage of the disease from other conditions that can cause abnormal topographic patterns, including corneal warpage due to contact lens wear, a prominent tear meniscus, dry eye disease with poor precorneal tear film, misalignment of the eye during obtaining the topography, displaced apex syndrome, and unintentional external pressure on the eye. The contact lens-induced cornea warpage can linger for quite a long period.

Forme Fruste Keratoconus

Forme fruste keratoconus which was first introduced by Amsler in 1961 is described as the fellow eyes of unilateral keratoconus with no clinical findings (corneal thinning, Fleischer's ring, or Vogt's striae), scissoring on retinoscopy, or any significant topographic changes such as inferior steepening.

Subclinical Keratoconus

Subclinical keratoconus is defined as the fellow eyes of unilateral keratoconus that have no history of ocular trauma, ocular surgery, contact lens wear, or slit-lamp or clinical findings (retinoscopic, keratometric, or biomicroscopic) of keratoconus but demonstrate inferior steepening or asymmetric bowtie pattern with SRAX in corneal topography.

Keratoconus Suspect

This term should appropriately be reserved for corneas that have no manifestation of clinical keratoconus in either eye but demonstrates subtle changes in corneal topography, including a localized area of inferior steepening, or an asymmetrical, truncated or skewed-axis bowtie.

Computerized Corneal Topography for the Diagnosis of Keratoconus

Corneal topography is an essential tool to perform the evaluation in refractive surgery preoperatively; it presents the curvature properties of the anterior corneal surface and is used to measure and evaluate its pattern and profile. The advances in corneal refractive surgery techniques have made it necessary to precisely analyze the topographic features of the cornea and differentiate normal corneas from the diseased ones to avoid iatrogenic ectasia postoperatively. Subclinical keratoconus, which is the most important risk factor for the development of post-refractive surgery ectasia, is usually asymptomatic and can be undiagnosed in a routine ophthalmic examination. The conventional keratometer only determines an estimation of the anterior corneal power at the paracental area but is inappropriate for the evaluation of candidates for refractive surgery. Recently, rapid advances in corneal imaging techniques have paralleled those of corneal refractive surgery, and evaluation of the cornea by computerized topography has become the standard

preoperative evaluation in clinical practice. The main purpose of this evaluation is to diagnose epithelial irregularities and stromal abnormalities, measure corneal astigmatism, and determine refractive stability or undiagnosed corneal diseases, such as forme fruste keratoconus, and pellucid marginal degeneration. Computerized topography provides three different data sets, including keratometric data, statistical indices, and map patterns.

Keratometric Data

Keratometric measurement provides a good accuracy in diagnosing keratoconus. Central keratometry is the mean value of corneal power for the areas with diameters of 2, 3 and 4 mm. A central keratometry between 47.2 D and 48.7 D is suggestive of keratoconus and a central keratometry larger than 48.7 diopters indicate clinical manifest keratoconus. In addition, a difference in central keratometry >1.0 D between two eyes is considered for differentiating subclinical keratoconus and normal eyes.

Maximum keratometry refers to the power of a point in the cornea that has the greatest power. This point can be inside or outside the central area. Minimum keratometry refers to the power of a point in the cornea that has the lowest power and can be inside or outside the central area.

Simulated keratometry is similar to the measurement achieved by manual keratometry and indicates the corneal power of the flat and steep meridian at the 3-mm paracentral area. If these two meridians are not perpendicular, the machine measures the magnitude of the steep meridian and that of 90 degrees apart from the steep meridian. Mean simulated keratometrty is the average of these two measurements and keratometric astigmatism is the difference between these two measurements. Astigmatism has been shown to be higher in keratoconus. Keratometric astigmatism of >1.5 D has an acceptable ability for the screening of keratoconus.

Statistical Indices

Corneal topography provides several quantitative indices which can be used to screen for keratoconus. These indices are either simple that evaluate one parameter or combined that use multivariate combinations of the topographic indices to provide one index. Simple indices include surface asymmetry index (SAI), surface regularity index (SRI), predicted visual acuity (PVA), Inferior–superior (I–S) value, irregular astigmatism index (IAI), opposite sector index (OSI), differential sector index (DSI), central/surround index (CSI), average central dioptric power (ACP), and analyzed area (AA). Combined indices include keratoconus severity index (KSI), keratoconus prediction index (KPI), and keratoconus percentage index (KPI). The combined indices are calculated using artificial neural networks.

Simple Indices

SAI is an index that shows a mean value of the power differences among the points spatially located at 180° from 128 equidistant meridians. A radially symmetrical optical surface has a SAI value of zero, and this value increases as the amount of asymmetry increases. A SAI value >0.5 is considered abnormal.

SRI is a local descriptor of regularity in a central zone of 4.5 mm of diameter that consists of the central ten rings of Placido disc. This index measures power gradient differences between successive pairs of rings in 256 equidistant semi-meridians and has good correlation with the visual acuity. A SRI value >1 is considered abnormal.

I–S value, which computes the vertical gradient cornea power of 6 mm region (inferior-superior dioptric asymmetry), is the refractive power difference between the 5 inferior points and the 5 superior points of the corneal area located at 3 mm from the corneal apex at 30 degree intervals. A negative value indicates steeper superior curvature while a positive value indicates steeper inferior curvature. An I–S value between 1.4 and 1.8 D suggests a keratoconus suspect, while a greater value suggests clinical keratoconus.

Relative skewing of the steepest radial axes above and below the horizontal meridian (SRAX) is defined as the angle between the orientation of more curved superior hemi-meridian and that of more curved inferior hemi-meridian and is an index that reflects the irregular astigmatism. An asymmetric bowtie pattern with a SRAX >21 degrees on corneal topography has a high accuracy in detecting keratoconus-affected corneas. This value is only important if keratometric astigmatism is >1.5 D. It has been found that a central keratometry >47.20 D, I–S higher than 1.5 D and SRAX index above 21° can identify 98% of the patients with keratoconus.

IAI is a measure of dioptric variables along each hemi-meridian, which is normalized by the number of measured points and the mean corneal power. An IAI value of >0.5 is considered an abnormality thresholds of keratoconus.

AA is the ratio of the area analyzed to the area circumscribed by the outermost peripheral ring.

CSI is an index that quantifies the average power difference between the central area of 3 mm diameter and a half-peripheral ring that is 3 and 6 mm diameters. CSI >1.0 is considered abnormal.

DSI is another index indicating the average power difference between sectors of 45° with the lowest and highest power. A DSI value > 3.50 is considered abnormal.

OSI is an index that quantifies average power difference between opposing sectors of 45°. A value of >2.10 is considered abnormal.

Combined Indices

Keratoconus prediction index (KPI) is a linear discriminate analysis of eight quantitative topographic indices from videokeratography to detect keratoconus. These

indices include simulated K1, simulated K2, SAI, CSI, DSI, OSI, IAI and AA. A KPI score >0.23 is suggestive of keratoconus. However, it is not always useful for the screening of keratoconus suspect because it has a significant overlapping between keratoconus suspect and keratoconus in its scoring system. This index has a sensitivity of 68% and a specificity of 99% for the detection of keratoconus.

KCI, also known as the Klyce-Maeda method, is derived by using a binary decision-making tree and linear discriminant analysis of eight indices obtained by the corneal topogrpahy. This method can discriminate a keratoconic cornea from a normal cornea. A KCI value of >0 is suggestive of keratoconus.

KSI, also known as the Smolek-Klyce method, is an index derived from neural network algorithm using ten topographic indices as inputs. This multivariate system computes the severity of keratoconus, which possibly differentiates among a normal cornea, a suspected keratoconic cornea and a keratoconus-affected cornea. A KSI value of less than 15% is considered normal, values between 15 and 30% as keratoconus suspect, and above this value is considered clinical keratoconus.

The KISA% index provides an algorithm to quantify outputs from corneal topography and is computed from four indices as follows;

$$\text{KISA\%} = \frac{(\text{K}) \times (\text{I} - \text{S}) \times (\text{AST}) \times (\text{SRAX}) \times 100}{300}$$

where, K is central keratometry value, I–S is inferior to superior value, AST is the regular astigmatism (difference between the magnitude of the steepest and flattest simulated keratometry), and SRAX is the skewed radial axis index (an expression of irregular astigmatism). This index is highly sensitive and specific in differentiating a healthy cornea from a keratoconus-affected cornea. A value of between 60 and 100% represents keratoconus suspect and that greater than 100% is highly suggestive of clinical keratoconus with minimal overlapping with normal corneas. This index, however, has a major drawback in its use as a tool for screening keratoconus in refractive surgery candidates because it has a significant number of false negatives. The abovementioned neural network systems are the 3 most widely used diagnostic systems based on corneal topography to differentiate healthy cornea, keratoconus suspect, subclinical keratoconus, and clinical keratoconus.

Topographic Maps

Different colors are used to represent dioptric values in the topographic map: cooler colors illustrate flatter curvatures (lower power), and warmer colors exhibit steeper curvatures (higher power). Ten different topographical patterns are proposed by Rabinowitz et al. in 1996, based on the quantitative indices and database of videokeratography patterns in the 390 corneas of normal subjects. These patterns include round, oval, superior steepening, inferior steepening, irregular, symmetric bowtie, symmetric bowtie with SRAX, asymmetric bowtie with inferior

steepening, asymmetric bowtie with superior steepening, and asymmetric bowtie with SRAX (Fig. 5). These patterns have different distribution in the normal population: round pattern 22.6%, oval pattern 20.8%, symmetric bowtie pattern 17.5%, asymmetric bowtie pattern 32.1%, and irregular pattern 7.0%. Some of these patterns are associated with normal corneas and the others are abnormal and indicate corneal diseases. Recently, 3 additional patterns related to pellucid marginal degeneration were added. These patterns include butterfly, crab claw, and junctional (Fig. 5).

Round pattern indicates a normal cornea with no significant astigmatism. This pattern is located centrally and the amount of displacement from the corneal center is less than 1 mm. However, it should be noticed that central keratoconus may have nipple cones with a diameter of $\leq$5 mm and are located in the center or slightly below the center of the cornea. In this situation, central keratometry is abnormally high.

Oval pattern indicates a normal cornea with an insignificant amount of astigmatism. This pattern is rarely encountered in keratoconus-affected corneas; in this situation, the pattern may displace inferotemporally or inferonasally.

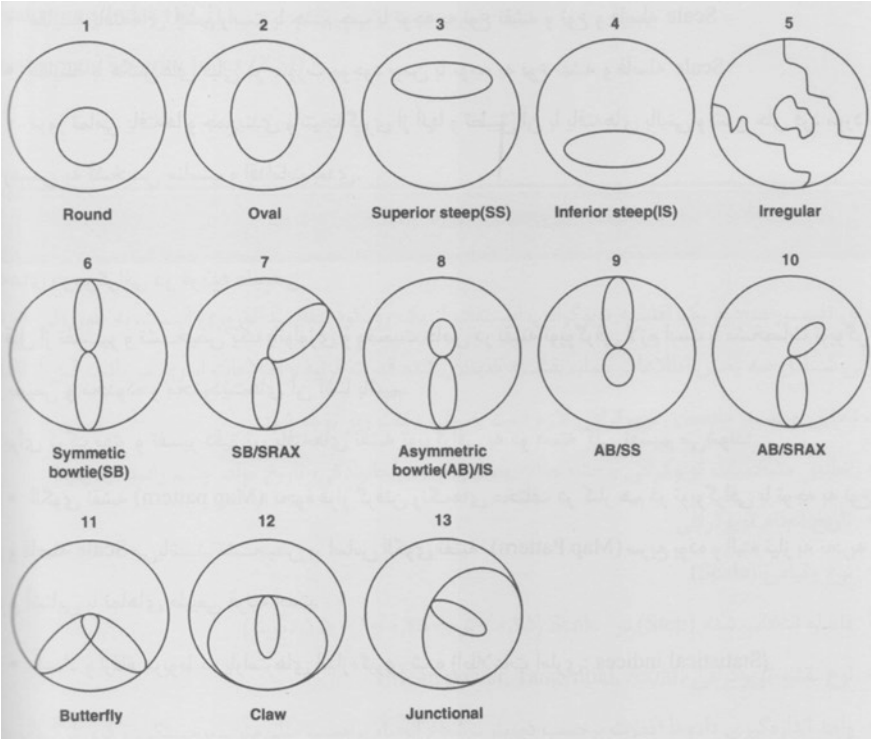

Fig. 5 Different topographical patterns of cornea

In the superior steepening pattern, the steepest area is located superiorly. Inferior corneal steepening is the most common pattern encountered in keratoconus (approximately 80% of keratoconus patients). In this pattern, the steepest area is located inferior or inferotemporal to the corneal center.

Irregular pattern demonstrates steep and flat areas with random distribution. This pattern is encountered in corneal opacities, corneal scars due to trauma, and after corneal transplantation.

Symmetric bowtie pattern which indicates regular astigmatism is located vertically, horizontally, or obliquely, depending on the type of astigmatism. Rarely, this pattern can be encountered in central keratoconus. In this situation, however, the size of the bowtie is small and the power of the cornea is abnormally high.

Symmetric bowtie pattern with SRAX indicates a non-orthogonal (irregular) astigmatism. The two segments are equal but not aligned. SRAX >21 degrees is highly suggestive of keratoconus in a cornea with astigmatism >1.5 D.

Asymmetric bowtie pattern with inferior steepening has two segments that are different in size, shape, and power, and the larger segment is located inferiorly. The vertical asymmetry is defined as the difference between the average inferior and the average superior values at the 5-mm central ring (the second circle of numbers) greater than 1.5 D. In asymmetric bowtie with superior steepening, the superior part of the bowtie is larger or more powerful than the inferior part and the difference between the average superior and the average inferior values at the 5-mm central ring is greater than 2.5 D.

Asymmetric bowtie pattern with SRAX has two different segments which are not aligned. This pattern is considered as abnormal when the angle between the axes of the superior and inferior segments in the innermost circle (3 mm) is more than 21 degrees and simulated keratometric astigmatism is greater than 1.5 D.

The butterfly and crab claw (kissing birds) patterns which are encountered in pellucid marginal degeneration indicate an against-the-rule astigmatism.

Case Presentation

Case 1

A 32 year-old man has a manifest refraction of $-3.5\ -4.25 \times 15^{\circ}$ OD and $-2.75\ -4.50 \times 160^{\circ}$ OS. Best-spectacle corrected visual acuity is 20/20 OU. Corneal topography demonstrates a symmetric bowtie pattern in both eyes. Corneal astigmatism is with-the-rule which means the orientation of astigmatism is between 60 and 120 degrees. The superior and inferior segments of the bowties have similar power, size, and shape, and there is no skew in their alignment, indicating regular astigmatism in these eyes. Please, note the presence of corneal enantiomorphism which means mirror symmetry in topographic patterns between the right and left corneas.

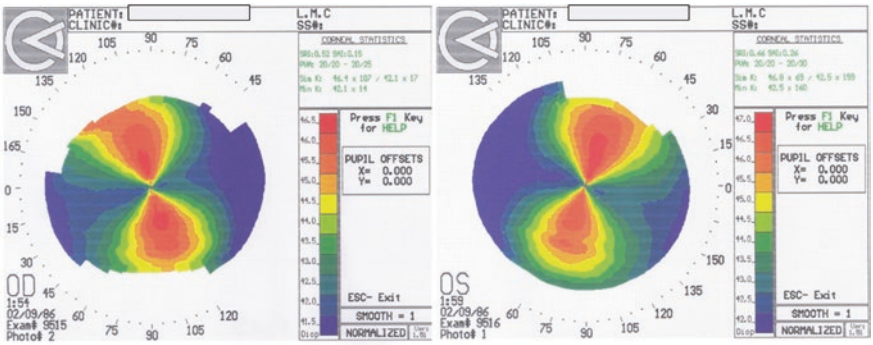

Case 2

A 54 year-old man has a manifest refraction of -1.75 $-2.0 \times 100°$ OD and -2.0 $-1.5 \times 80°$ OS. Best-spectacle corrected visual acuity is 20/20 OU. Corneal astigmatism is oriented horizontally (against-the-rule astigmatism). The corneal topography demonstrates an asymmetric bowtie pattern as the size of the temporal segment is greater than that of the nasal segment. Please, note the presence of corneal enantiomorphism which means mirror symmetry in topographic patterns between the right and left corneas.

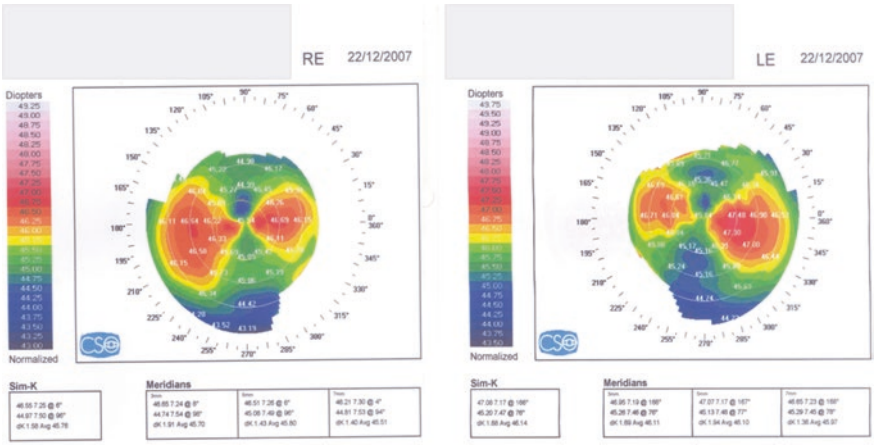

Case 3

A 30 year-old woman was examined for refractive surgery. Best-spectacle corrected visual acuity was 20/20 OD with $-4.25\ -0.50 \times 110°$. Central corneal thickness measured using an ultrasonic pachymetry was 498 microns in this eye. In the corneal topography, keratometric measurements are normal and all simple and combined indices, except for different sector index, are within the normal range; however, an inferior steepening is evident in the color-coded map. Similar findings were found in the fellow eye. The patient was diagnosed with keratoconus suspect and the surgery was cancelled.

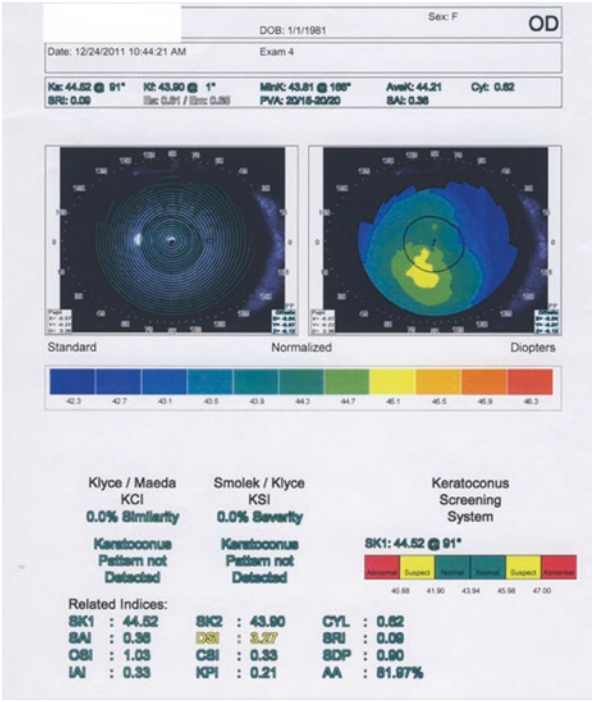

Case 4

A 36 year-old woman has a manifest refraction of $-6.0\ -1.0 \times 25°$ OD and -5.75 OS with a best-spectacle corrected visual acuity of 20/20 OU. Topographic patterns are asymmetric bowtie without SRAX. Please, note some indices are suspect (highlighted in yellow) and some indices are abnormal (highlighted in red).

Despite these findings, keratoconus index and keratoconus severity index are interpreted normal. The patient is diagnosed with keratoconus suspect.

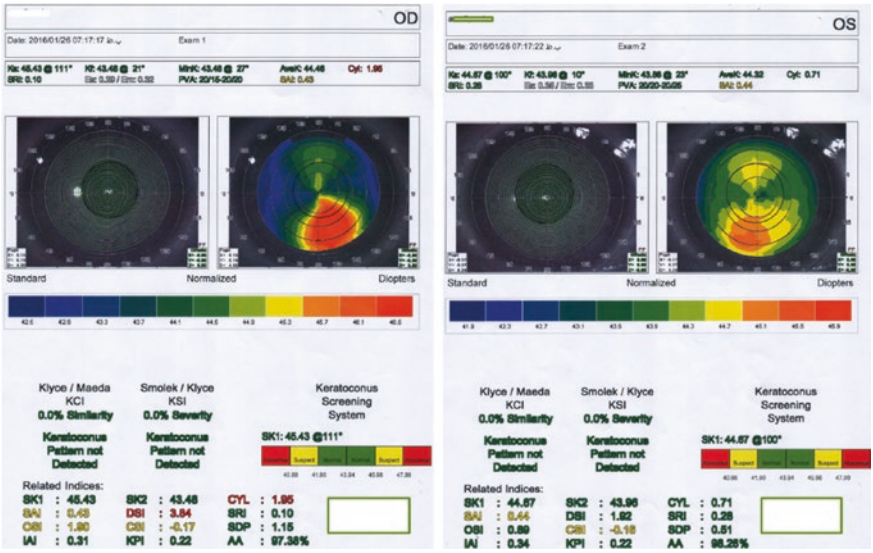

Case 5

A 21 year-old woman has a manifest refraction of $-4.75\ -2.50 \times 20°$ with a best-spectacle corrected visual acuity of 20/20 OS. Corneal topography demonstrates asymmetric bowtie with superior steepening. Some statistical indices are suspect and some are abnormal. Please, note keratoconus suspect is interpreted by the keratoconus severity index.

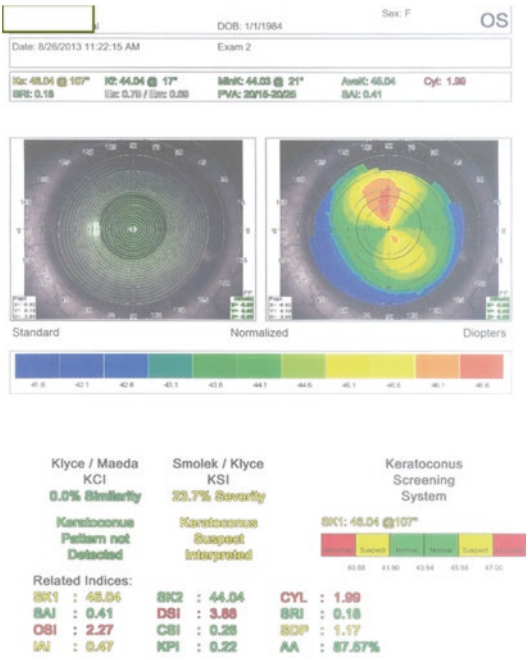

Case 6

A 24 year-old keratoconus-affected woman has a manifest refraction of −5.0 −7.5 × 30° and best-spectacle corrected visual acuity of 20/60 OD. Corneal topography reveals that all keratometric measurements and statistical indices are abnormally high. Topographic pattern is asymmetric bowtie with inferior steepening. Please, note the presence of SRAX

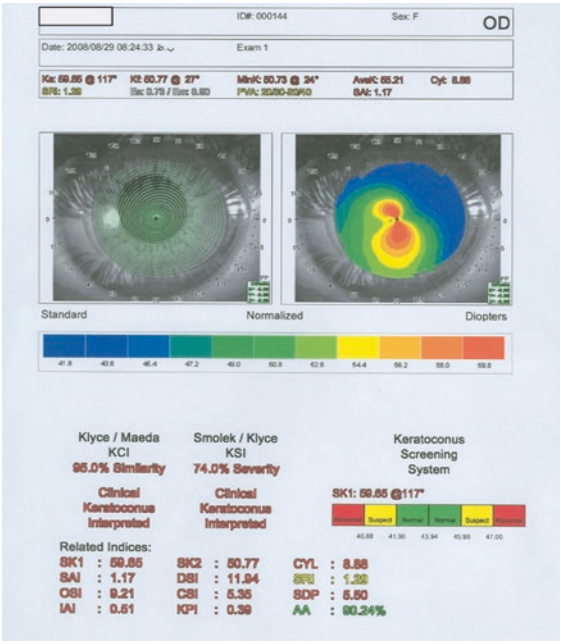

Case 7

A 51 year-old man has a manifest refraction of $-3.0\ -5.75 \times 70^{\circ}$ with a best-corrected visual acuity of 20/60 OD. The corneal topography demonstrates an against-the-rule irregular astigmatism with a crab claw pattern. The patient is diagnosed with pellucid marginal degeneration.

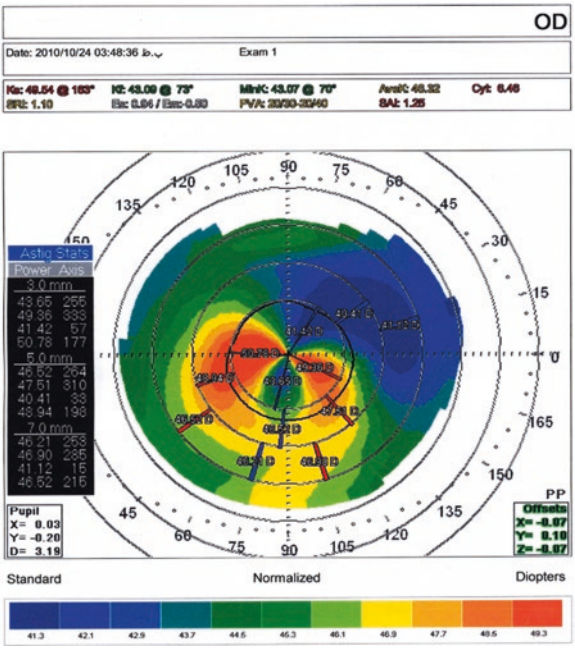

References

1. Anderson D, Kojima R. Topography: A clinical pearl. Optom Manag. 2007;42:35.
2. de Sanctis U, Aragno V, Dalmasso P, Brusasco L, Grignolo F. Diagnosis of subclinical keratoconus using posterior elevation measured with 2 different methods. Cornea. 2013;32:911–5.
3. Gatinel D. Corneal topography and wave front analysis. In: Albert & Jakobiec's principles & practice of ophthalmology, 3rd ed. Philadelphia, PA: Saunders/Elsevier; 2008. p. 921–963.
4. Gatinel D, Malet J, Hoang-Xuan T, Azar DT. Corneal elevation topography: best fit sphere, elevation distance, asphericity, toricity and clinical implications. Cornea. 2011;30:508–15.
5. Kanellopoulos AJ, Asimellis G. OCT-derived comparison of corneal thickness distribution and asymmetry differences between normal and keratoconic eyes. Cornea. 2014;33:1274–81.
6. Kim E, Weikert MP, Martinez CE, Klyce SD. Keratometry and topography. In: Cornea, 4th ed. Holland: Elsevier; 2017. p. 144–153.
7. Martínez-Abad A, Piñero DP. New perspectives on the detection and progression of keratoconus. J Cataract Refract Surg. 2017;43:1213–27.
8. Muftuoglu O, Ayar O, Ozulken K, Ozyol E, Akıncı A. Posterior corneal elevation and back difference corneal elevation in diagnosing forme fruste keratoconus in the fellow eyes of unilateral keratoconus patients. J Cataract Refract Surg. 2013;39:1348–57.
9. Naroo SA, Cervino A. Corneal topography and its role in refractive surgery. In: Refractive surgery: a guide to assessment and management. London, UK: Elsevier; 2004. p. 9–16.

10. Placido A. Novo instrumento per analyse immediate das irregularitades de curvatura da cornea. Periodico Oftalmol Practica. 1880;6:44–9.
11. Prakash G, Agarwal A, Mazhari AI, Kumar G, Desai P, Kumar DA, Jacob S, Agarwal A. A new, pachymetry-based approach for diagnostic cutoffs for normal, suspect and keratoconic cornea. Eye. 2012;26:650–7.
12. Rabinowitz YS. Videokeratographic indices to aid in screening for keratoconus. J Refract Surg. 1995;11:371–9.
13. Rabinowitz YS1, Yang H, Brickman Y, Akkina J, Riley C, Rotter JI, Elashoff J. Videokeratography database of normal human corneas. Br J Ophthalmol. 1996;80:610–6.
14. Randleman JB, Russell B, Ward MA, Thompson KP, Stulting RD. Risk factors and prognosis for corneal ectasia after LASIK. Ophthalmology. 2003;110:267–75.
15. Randleman JB, Woodward M, Lynn MJ, Stulting RD. Risk assessment for ectasia after corneal refractive surgery. Ophthalmology. 2008;115:37–50.
16. Reddy JC, Rapuano CJ, Cater JR, Suri K, Nagra PK, Hammersmith KM. Comparative evaluation of dual Scheimpflug imaging parameters in keratoconus, early keratoconus, and normal eyes. J Cataract Refract Surg. 2014;40:582–92.
17. Salz JJ, Trattler W. Patient evaluation and selection in refractive surgery. In: Cornea, 4th ed. Holland: Elsevier; 2017. p. 1719–27.
18. Santhiago MR, Smadja D, Gomes BF, Mello GR, Monteiro ML, Wilson SE, Randleman JB. Association between the percent tissue altered and post-laser in situ keratomileusis ectasia in eyes with normal preoperative topography. Am J Ophthalmol. 2014;158:87–95.
19. Schallhorn JM, Tang M, Li Y, Louie DJ, Chamberlain W, Huang D. Distinguishing between contact lens warpage and ectasia: Usefulness of optical coherence tomography epithelial thickness mapping. J Cataract Refract Surg. 2017;43:60–6.
20. Smadja D. Topographic and tomographic indices for detecting keratoconus and subclinical keratoconus: a systematic review. Int J Keratoconus Ectatic Corneal Dis. 2013;2:60–4.
21. Tanuj D, Neha M, Tarun A. New investigations in ophthalmology, vol. 3, 2nd ed. 2017. p. 30.
22. Taravella M, Davidson RS. Corneal topography and Wavefront Imaging. In: Ophthalmology, 4th ed. Philadelphia, PA: Saunders/Elsevier; 2014. p. 168–73.
23. Toprak I, Yaylalı V, Yildirim C. A combination of topographic and pachymetric parameters in keratoconus diagnosis. Cont Lens Anterior Eye. 2015;38:357–62.
24. Yeu E, Belin MW, Khachikian SS. Topographic analysis in keratorefractive surgery. In: Cornea, 4th ed. Holland: Elsevier; 2017. p. 1728–35.